

Two-particle dispersion in model two-dimensional velocity fields

I.M. Sokolov^a

Theoretische Polymerphysik, Universität Freiburg, Hermann-Herder-Str. 3, 79104 Freiburg, Germany

Received 13 March 2001

Abstract. We consider two-particle dispersion in a velocity field, where the relative two-point velocity scales according to $v^2(r) \propto r^\alpha$ and the corresponding correlation time scales as $\tau(r) \propto r^\beta$, and fix $\alpha = 2/3$, as typical for turbulent flows. We show that two generic types of dispersion behavior arise: For $\alpha/2 + \beta < 1$ the correlations in relative velocities decouple and the diffusion approximation holds. In the opposite case, $\alpha/2 + \beta > 1$, the relative motion is strongly correlated. The case of Kolmogorov flows corresponds to a marginal, nongeneric situation. In this case, depending on the particular parameters of the flow, the dispersion behavior can be rather diffusive or rather ballistic.

PACS. 05.40.-a Fluctuation phenomena, random processes, noise, and Brownian motion – 47.27.Qb Turbulent diffusion

Since the seminal article of Sir L.F. Richardson on the particles' dispersion in atmospheric turbulence [1] a large amount of work has been done in order to understand the fundamentals of this process (see [2] and [3] for reviews). Based on an empirical evidence, Richardson found out that the mean square distance $R^2(t) = \langle r^2(t) \rangle$ between the two particles dispersed by a turbulent flow grows proportionally to t^3 . The works of Obukhov and Batchelor have shown that the Richardson's law is closely related to the Kolmogorov-Obukhov scaling of the relative velocities in turbulent flows. Scaling arguments based on the dimensional analysis allow then to understand the overall type of the behavior of $R^2(t)$. Thus, the Richardson's law follows as an intermediate asymptotic behavior pertinent to the inertial range $\lambda \ll R \ll L$, where λ is the viscous scale and L is the integral scale of the flow. On the other hand, the full theoretical picture of the dispersion process is still lacking, and typical analytical results disagree strongly with those of experiments and simulations [3]. Thus much effort was put into development of stochastic approaches which do not follow directly from equations of fluid dynamics but use extra physical assumptions.

The theoretical description of the dispersion process typically starts from models, in which one fixes the spatial statistics of the well developed turbulent flow (Kolmogorov-Obukhov energy spectrum), and discusses different types of the flows' temporal behavior [3]. Three situations have been considered so far. In connection with "real" turbulence the two cases are widely discussed. They correspond to different assumptions about the life-time of the flow structures ("eddies") and about their transport

by the overall flow. In one of them the temporal decorrelation is connected with death and birth of the eddies, whose lifetime is proportional to their revolution time and is governed by the Kolmogorov's universality assumption [4, 5]. Another premise supposes that the temporal decorrelation of the particles' relative motion takes place because the pair as a whole is moving, due to a mean velocity, relative to an essentially frozen flow structure (as proposed by a Taylor hypothesis, see Sect. 21.4 of Ref. [2]). This assumption serves as a basis for successful numerical approaches [5, 6], see Section 6.5.1 of reference [3] for discussion. Thus, in applications the time-dependent turbulent flow is often mimicked either by sweeping a frozen array of eddies past the laboratory frame by some constant velocity [6] or by sweeping indefinitely persisting eddies by the overall (self-consistent) velocity field [7]. Both Kolmogorov and Taylor situations are extremely awkward for theoretical analysis. On the other hand, the white-in time flows represent a toy model which allows for deep analytical insights [8, 9].

In the present note we address the following question: What are the generic types of the two-particle dispersion behavior in a velocity field whose statistical spatial structure is fixed (and similar to one of a turbulent flow), if its temporal correlation properties change. To answer this question we present a tunable model that covers the overall range of interest and discuss the situation in the framework of scaling concepts and numerical simulations. As we proceed to show, two generic types of behavior arise. Thus, the white-in-time flow and the Taylor-type situation belong to the classes of diffusive and ballistic behavior, respectively. The case of Kolmogorov temporal scaling represents a borderline situation, in which case, depending

^a e-mail: igor@tpoly.physik.uni-freiburg.de

on the particular parameters of the flow, the dispersion behavior can be rather diffusive or rather ballistic. The properties of this nongeneric case can hardly be understood without deep understanding of generic patterns.

Let us consider modes of particles' separation in a velocity field whose two-time correlation function of relative velocities behaves as $\langle \mathbf{v}(\mathbf{r}, t_1) \mathbf{v}(\mathbf{r}, t_2) \rangle \propto \langle v^2(r) \rangle g[(t_2 - t_1)/\tau(r)]$, where $\tau(r)$ is the distance-dependent correlation time. The g -function is defined so that $g(0) = 1$ and $\int_0^\infty g(s) ds = 1$. The mean square relative velocity and the correlation time scale as

$$\langle v^2(r) \rangle \propto v_0^2 \left(\frac{r}{r_0} \right)^\alpha \quad (1)$$

and

$$\tau(r) \propto \tau_0 \left(\frac{r}{r_0} \right)^\beta. \quad (2)$$

One can visualize such a flow as being built up from several structures (plane waves, eddies, etc., see Ref. [3]), each of which is characterized by its own spatial scale and its scale-dependent correlation time. In well-developed turbulent flows the Kolmogorov scaling postulate [10] implies that the energy dissipation rate ϵ (having the dimension of $[L^2/T^3]$) is the only relevant dimensional parameter in the inertial range, so that one has $v^2(r) \propto \epsilon^{2/3} r^{2/3}$ and $\tau \propto \epsilon^{-1/3} r^{2/3}$, so that $\alpha = 2/3$ and $\beta = 2/3$. The simplifying assumptions disregard the connection between α and β . Thus, the Taylor's frozen-flow assumption leads to $\beta = 1$, and the white-in-time flow corresponds to $\beta = 0$. In what follows we discuss the behavior of two-particle separation for different values of $\beta \in [0, 1]$ in a two-dimensional system in order to identify the generic regimes and pay special attention to a Kolmogorov case as one of the most experimental relevance.

Although three-dimensional synthetic turbulent flows can be readily generated [3], there are several reasons to restrict ourselves to two-dimensional flows. First, the two-dimensional results are of immediate experimental relevance. Thus 2d flows generated by inverse energy cascade show the same Kolmogorov scaling behavior as 3d ones in the direct cascade case. This behavior was theoretically predicted in late 1960s [11,12] and observed experimentally [13]. The details of such velocity fields are easily accessible for measurements and allow direct comparison with simulations. On the other hand, in 2d it is considerably easier to collect the data statistics large enough to enable detection of rare events, possibly of high importance in dispersion process [6,14,15]. In our simulations we use the quasi-Lagrangian approach of reference [4]. The relative velocity $\mathbf{v}(\mathbf{r}, t) = \nabla \times \eta(\mathbf{r}, t)$ is given by the quasi-Lagrangian stream function η . This function is built up from the contributions of radial octaves:

$$\eta(\mathbf{r}, t) = \sum_{i=1}^N k_i^{-(1+\alpha/2)} \eta_i(k_i \mathbf{r}, t), \quad (3)$$

where $k_i = 2^i$, and the flow function for one-octave contribution in polar coordinates (r, θ) is given by

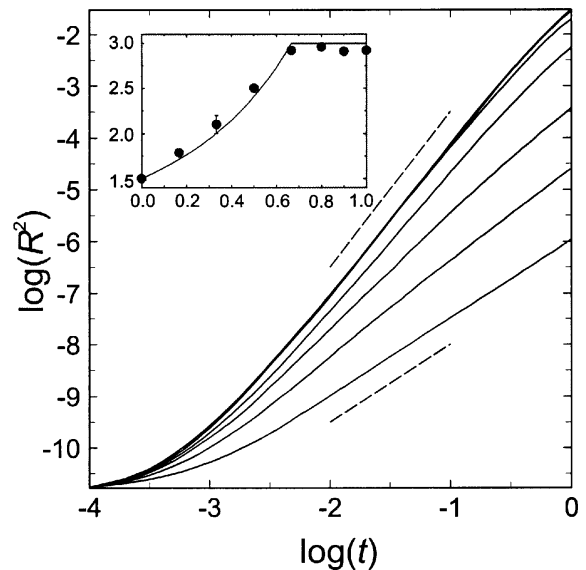


Fig. 1. Mean square displacement $R^2(t)$ plotted in double logarithmic scales. The four lower curves correspond to $\beta = 0, 0.17, 0.33$ and 0.5 (from bottom to top). The dashed lines indicate the slopes 1.5 and 3. The four upper curves for $\beta = 0.67, 0.8, 0.9$ and 1 are hardly distinguishable within the statistical errors of the simulations. The inset shows the values of $\gamma(\beta)$. The error bar shows the typical accuracy of all γ -values. The full lines give the theoretical predictions, equations (4, 5).

$\eta_i(k_i \mathbf{r}, t) = F(k_i r) (A_i(t) + B_i(t) \cos(2\theta + \phi_i))$. The radial part $F(x)$ obeys $F(x) = x^2(1-x)$ for $0 \leq x \leq 1$ and $F(x) = 0$ otherwise, and ϕ_i are quenched random phases. The choice of η_i proposed in [4] is not arbitrary but is based on the lowest-order perturbation expansion of the generic quasi-Lagrangian stream function for r small. Moreover, $A_i(t)$ and $B_i(t)$ are independent Gaussian random processes with $\langle A_i(t) \rangle = \langle B_i(t) \rangle = 0$ and $\langle A_i^2(t) \rangle = \langle B_i^2(t) \rangle = v_0^2$, and with correlation times $\tau_i = 2^{-i\beta} \tau_0$. At each time step these processes are generated according to $X_i(t + \Delta t) = \sqrt{1 - (\Delta t/\tau_i)^2} X_i(t) + (\Delta t/\tau_i) v_0^2 \zeta$, where X is A or B , and ζ is a Gaussian random variable with zero mean and unit variance. The values of τ_0 and the integration step Δt are to be chosen in such a way that $\tau_N \gtrsim \Delta t$. Typically, values of $\Delta t \sim 10^{-4}$ are used. For the noncorrelated flow ($\beta = 0$) the values of $A_i(t)$ and $B_i(t)$ are renewed at each integration step Δt . In the present simulations $N = 16$ was used. The value $v_0 = 1$ was employed in the majority of simulations reported here, so that only the use of a different v_0 value will be explicitly stated in the following.

The values of $R^2(t)$ obtained from 3000 realizations of the flow for several values of $\beta \in [0, 1]$ are plotted on double logarithmic scales in Figure 1, where $\tau_0 = 0.15$ is used. One can clearly see that for all β a scaling regime $R^2(t) \propto t^\gamma$ appears. We note moreover that the curves for $\beta = 0.67, 0.8, 0.9$ and 1.0 are almost indistinguishable within statistical errors. The values of γ as a function of β are presented in the inset, together with the theoretically predicted forms, vide infra. These values are determined by a least-squares-fit within the scaling region of

each curve: the values shown are obtained in the domain $-2 \leq \log_{10} t \leq 0$ for $\beta = 0$ and for $\beta = 0.17$, and in the domain $-2.5 \leq \log_{10} t \leq -0.5$ for the other values of β . The uncertainty in the values of γ (indicated as a typical error bar) is mostly connected with the choice of fitting region.

The regimes of dispersion found in simulations can be explained within the framework put forward in reference [16]. The discussion starts by considering $l(r) = v(r)\tau(r)$, the mean free path of motion at the distance r . If this mean free path always stays small compared to r , the relative motion exhibits a diffusive behavior with a position-dependent diffusion coefficient, $K(r) \propto l^2(r)/\tau(r) \propto r^{\alpha+\beta}$. Taking as a scaling assumption $r \propto \langle r^2(t) \rangle^{1/2} = R$, one gets that the mean square separation R grows as $R^2 \propto t^\gamma$ with

$$\gamma = \frac{2}{2 - (\alpha + \beta)}. \quad (4)$$

On the other hand, if $l(r)$ is of the order of r , the mean separation follows from the integration of the ballistic equation of motion $\frac{d}{dt}R = v(R) \propto R^{\alpha/2}$, see reference [15]. Thus, in a flow where a considerable amount of flow lines of relative velocity are open, one gets $R^2 \propto t^\gamma$, with

$$\gamma = \frac{4}{2 - \alpha}. \quad (5)$$

The occurrence of either regime is governed by the value of the (local) persistence parameter of the flow,

$$Ps(r) = l(r)/r = v(r)\tau(r)/r. \quad (6)$$

Small values of Ps correspond to erratic, diffusive motion, while large values of Ps imply that the motion is strongly persistent. The value of the persistence parameter scales with r as $Ps(r) \propto r^{\alpha/2+\beta-1}$. Since under particle's dispersion the mean interparticle distance grows continuously with time, the value of Ps decreases continuously for $\alpha/2 + \beta < 1$, so that the diffusive approximation is asymptotically exact. For $\alpha/2 + \beta > 1$ the lifetimes of the structures grow so fast that the diffusive approximation does not hold. This situation is one observed in our simulations for $\beta > 2/3$. The strong ballistic component of motion implies that the velocities stay correlated over considerable time intervals. The results of Figure 1 confirm that $\gamma(\beta)$ behaves accordingly to equation (4) for $\beta < 2/3$ and equation (5) for $\beta > 2/3$. We note here that the parameters of the simulations presented in Figure 1 ($v_0 = 1$, $\tau_0 = 0.15$) were chosen in a way that allows to show all curves within the same time- and distance intervals. This leads to a somehow restricted scaling range and to slight overestimate of γ -values in the diffusive domain.

Strong differences between the diffusive and the ballistic regimes can be readily inferred when looking at typical trajectories of the motion, such as ones plotted in Figure 2 for the cases $\beta = 0.33$ and $\beta = 0.67$. The difference between the trajectories is evident both in the (x, y) -plots and in the $r(t)$ -dependences. The curves for

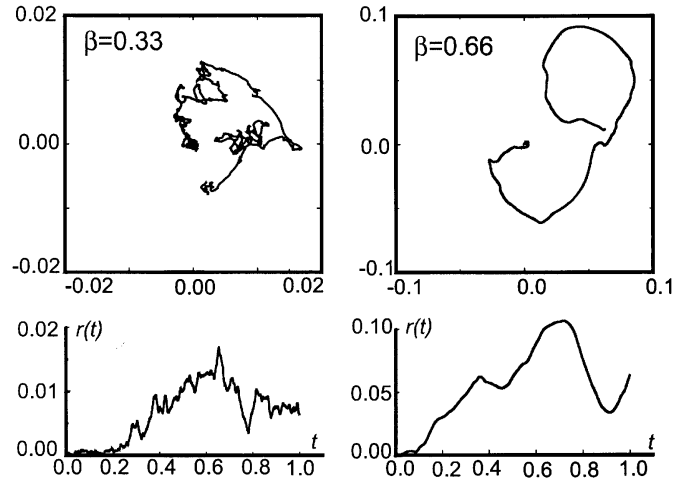


Fig. 2. Typical trajectories in the diffusive regime ($\beta = 0.33$) and in the Kolmogorov regime ($\beta = 0.67$). The upper pictures show the trajectories in the (x, y) -plane, the lower ones represent the corresponding $r(t)$ -behavior. Note that the scales of the right and of the left graphs differ by a factor of 5.

$\beta = 0.33$ exhibit a random-walk-like, erratic behavior, while the curves for $\beta = 0.67$ show long periods of laminar, directed motion. In order to quantitatively characterize the strength of the velocity correlations we calculate the backwards-in-time correlation function (BCF) of the radial velocities, as introduced in reference [13]. This function is defined as $C_r(\tau) = \langle v_r(t - \tau)v_r(t) \rangle / \langle v_r^2(t) \rangle$ and shows, what part of its history is remembered by a particle in motion. The function is plotted in Figure 3 against the dimensionless scaled time $\vartheta = -\tau/t$. The functions (obtained in 10^4 realizations each) are plotted for 4 different sets of parameters. Here the dashed lines correspond to $\beta = 0.33$, in the diffusive range, for $t = 10^{-2}$, 3×10^{-2} , 10^{-1} and 3×10^{-1} . These BCFs do not follow a universal law as functions of ϑ only, and are rather sharply peaked close to zero, thus indicating the loss of memory. The two sets of full lines indicate $C_r(\tau)$ in Kolmogorov flows, for $t = 10^{-2}$, 3×10^{-2} , and 10^{-1} . The lower set corresponds to the value $\tau_0 = 0.05$ and the upper set to the value $\tau_0 = 0.15$. In both cases the functions show universal behavior, *i.e.* follow the same pattern as a function of ϑ , independent of t . No considerable changes in the BCF's form occur when further increasing the value of τ_0 up to $\tau_0 = 1$, thus indicating that the data $\tau_0 = 0.15$ correspond already to a strongly correlated regime. The form of these curves resembles closely the experimental findings of reference [13]. The BCFs for $\beta = 1.0$ show an overall behavior very similar to the one in Kolmogorov's case. Note that as the time grows the curves for $\beta = 1.0$ approach those for $\beta = 2/3$ and probably tend to the same limit. The curves for $\beta = 1.0$ and $\tau_0 = 1$ (not shown) fall together with those in Kolmogorov's case with $\tau_0 = 0.15$.

The similarity in the properties of dispersion processes in a Kolmogorov situation with larger Ps (larger τ_0) and in ballistic regime can be explained based on the behavior of the effective persistence parameter. In the diffusive

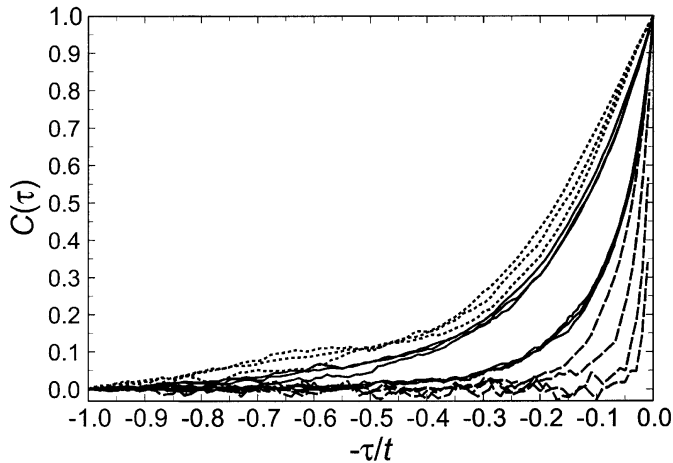


Fig. 3. The BCF of relative velocities as a function of the dimensionless time lag $-\tau/t$. The lower group of dashed lines corresponds to $\beta = 0.33$ (the values of t are 0.01, 0.03, 0.1 and 0.3, from top to bottom). The two groups of full curves corresponds to the Kolmogorov case (three curves for $t = 0.01, 0.03, 0.1$ each). The dotted curves correspond to $\beta = 1$ for the same values of time, see text for details.

regime we supposed that the correlation time of the particles' relative velocity scales in the same way as the Eulerian lifetime of the corresponding structures. On the other hand, in the ballistic regime, $\beta > 1 - \alpha/2$, the lifetimes of the structures grow so fast that no considerable decorrelation takes place during the time the particles sweep through the structure. The Lagrangian decorrelation process is then connected not to Eulerian decorrelation, but to sweeping along open flow lines. The effective correlation time then scales according to $\tau_s(r) \propto r/v(r) \propto t^{1-\alpha/2}$, and the effective value of β stagnates at $\beta = 1 - \alpha/2$. Thus, all long-time correlated cases belong to the same universality class of strongly-correlated flows, as the Kolmogorov flows with large Ps , for which equations (4, 5) coincide. Note that it does not mean that the properties of dispersion cease to depend on the temporal properties of the flow, as shown in reference [17] for the case of the model flow with $\beta = 2$.

For Kolmogorov flows the ballistic and the diffusive mechanisms lead to the same functional form of $R^2(t)$ -dependence [18]. The functional form of the dependence of $R^2(t)$ on parameters of the flow is $R^2 \propto (v_0^2 \tau_0 / r_0^{\alpha+\beta})^\gamma t^\gamma$ in the diffusive situation ($Ps \ll 1$) and $R^2 \propto (v_0 / r_0^{\alpha/2})^\gamma t^\gamma$ in the ballistic case ($Ps \gg 1$). Assuming that Ps is the single relevant parameter governing the dispersion we are lead to the form $R^2(t) \propto f(Ps) (v_0 / r_0^{\alpha/2})^\gamma t^\gamma$, where $f(Ps)$ is a universal function of Ps , which behaves as Ps^γ for $Ps \ll 1$ and tends to a constant for $Ps \gg 1$. Thus, for a fixed spatial structure of the flow, the following scaling assumption is supposed to hold:

$$\frac{R^2(t)}{(v_0 t)^\gamma} = F(v_0 \tau_0), \quad (7)$$

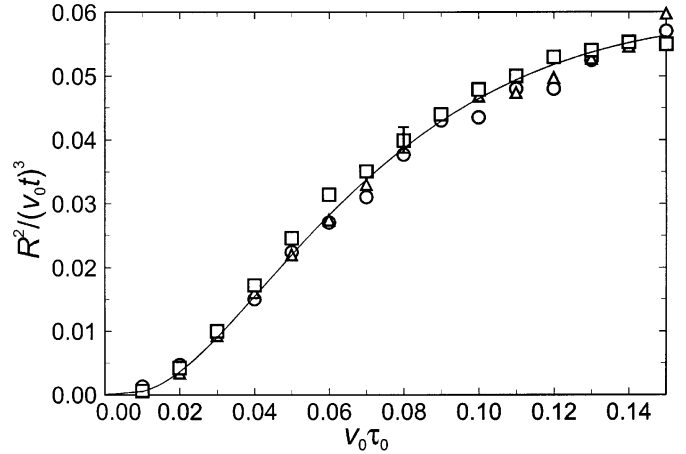


Fig. 4. The values of $R^2(t)/(v_0 t)^3$ plotted against $v_0 \tau_0$. The full line is drawn as a guide to the eye.

which scaling can be checked in our case by plotting $R^2(t)/(v_0 t)^3$ against $v_0 \tau_0$. The corresponding plot is given in Figure 4, where we fix $t = 0.1$, and plot the results in three series of simulations. Each point corresponds to an average over 5×10^4 runs. Here the squares correspond to $v_0 = 1$ and to the values of τ_0 ranging between 0.01 and 0.15, the triangles correspond to $v_0 = 0.3$ and to τ_0 between 0.033 and 0.5, and the circles to $\tau_0 = 0.1$ and to values of v_0 between 0.1 and 1.5. The error bar indicates a typical statistical error as inferred from 5 similar series of 5×10^4 runs each. The scaling proposed by equation (7) is well-obeyed by the results. Some points outside of the range of Figure 4 were also checked. Thus, for larger values of $v_0 \tau_0$ the values of $R^2(t)/(v_0 t)^3$ seem to stagnate. On the other hand, increasing $v_0 \tau_0$ to values larger than 0.3 (*i.e.* approaching the frozen flow regime) leads to a strong increase in fluctuations, making the results less reliable.

Another sign of the transition from diffusive to ballistic regime when increasing $v_0 \tau_0$ in the Kolmogorov flow is given by the distribution of the relative distances between the turning points of the trajectories of relative motion. The model of reference [18] proposes that for the flows following Kolmogorov scaling, the ratio of the positions of two subsequent turning points of the trajectory, r_1 and r_2 , $\xi = r_1/r_2$, has a probability density with the outer tail that scales as $p(\xi) \propto \xi^{-\lambda}$ (for $\xi > 1$) with $\lambda = 1 + 1/Ps$, so that the process leading to the turbulent dispersion can be described as a kind of multiplicative Lévy-process. The values of $\lambda > 3$ correspond to the diffusive behavior, while for $\lambda < 3$ a strong ballistic component is present. For $\lambda < 2$ even the first moment of the corresponding distribution is absent, and a considerable amount of particles reach the end of inertial range without changing once a direction of their relative motion.

In Figure 5 we plot on double logarithmic scales the probability density $p(\xi)$ as obtained in 10^6 realizations of the trajectories (as one shown in Fig. 2) for the Kolmogorov case for $v_0 = 1$ and different values of $\tau_0 = 0.02, 0.05, 0.2$ and 1.0. Figure 5 shows that the

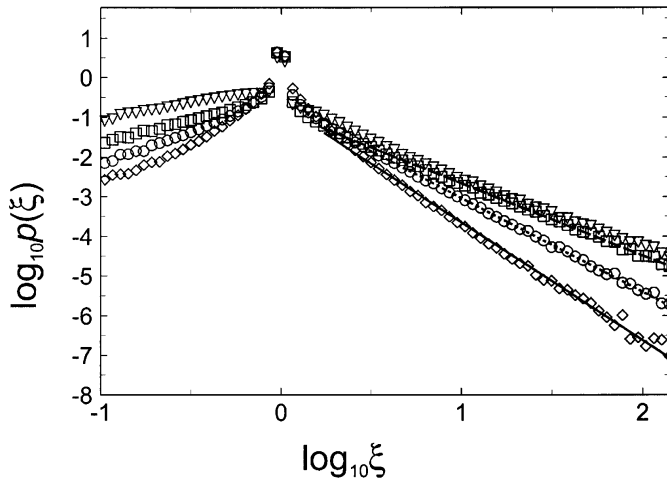


Fig. 5. The probability density of the distribution of the relative positions of two subsequent turning points of relative motion, $\xi = r_2/r_1$. Note the double logarithmic scales. The diamonds correspond to $\tau_0 = 0.02$, the circles to $\tau_0 = 0.05$, the squares to $\tau_0 = 0.2$, and the triangles $\tau_0 = 1.0$. The full, dotted and dashed lines have the slopes of -3.1 , -2.4 and -1.8 , respectively.

outer tail of $p(\xi)$ follows a power-law (a straight line on the scales of Fig. 5) and that the corresponding slope $-\lambda$ grows with τ_0 . Thus, the case $\tau_0 = 0.02$ corresponds to the diffusive behavior (the second moment of ξ exists), the case $\tau_0 = 0.05$ is one where the ballistic behavior gets important (the second moment of ξ diverges, but the first one still exists), and the cases $\tau_0 = 0.2$ and $\tau_0 = 1.0$ are dominated by ballistic events (the first moment of ξ diverges).

Let us summarize our findings. Thus, we considered two-particle dispersion in a velocity field scaling according to $v^2(r) \propto r^{2/3}$ and $\tau(r) \propto r^\beta$. We show that two generic types of behavior are possible: For $\alpha/2 + \beta < 1$ the diffusion approximation holds and the increase in the interparticle distances is governed by the distance-dependent diffusion coefficient $K(r) \propto r^{\alpha+\beta}$. In the opposite case $\alpha/2 + \beta > 1$ the relative velocities stay strongly correlated. The transition between the two regimes takes place

exactly for the Kolmogorov flow, for which $\alpha/2 + \beta = 1$. In this case the properties of the dispersion process depend on the persistence parameter of the flow.

The author is thankful to P. Tabeling, I. Procaccia, V. L'vov, J. Klafter, A. Blumen and G. Boffetta for enlightening discussions. Financial support by the Deutsche Forschungsgemeinschaft through the SFB 428 and by the Fonds der Chemischen Industrie is gratefully acknowledged.

References

1. L.F. Richardson, Proc. R. Soc. London, Ser. A **110**, 709 (1926).
2. A.S. Monin, A.M. Yaglom, *Statistical Fluid Mechanics* (MIT, Cambridge, MA, 1971), Vol. I; (1975), Vol. II.
3. A.J. Majda, P.R. Kramer, Phys. Rep. **314**, 237 (1999).
4. G. Boffetta, A. Celani, A. Crisanti, A. Vulpiani, Europhys. Lett. **42**, 177 (1999); Phys. Rev. E **60**, 6734 (1999).
5. F. Fung, J.C. Vassilicos, Phys. Rev. E **57**, 1677 (1998).
6. F.W. Elliot, A.J. Majda, Phys. Fluids **8**, 1052 (1996).
7. E.R. Abragam, Nature **391**, 577 (1998).
8. R.H. Kraichnan, Phys. Fluids **11**, 945 (1968); R.H. Kraichnan, Phys. Rev. Lett. **72**, 1016 (1994); R.H. Kraichnan, V. Yakhot, S. Chen, *ibid.* **75**, 240 (1995).
9. U. Frisch, A. Mazzino, M. Vergassola, Phys. Rev. Lett. **80**, 5532 (1998).
10. U. Frisch, *Turbulence* (Cambridge University Press, Cambridge, 1995), p. 100 ff.
11. R.H. Kraichnan, Phys. Fluids **10**, 1417 (1967).
12. C.E. Leith, Phys. Fluids **11**, 671 (1968).
13. M.C. Jullien, J. Paret, P. Tabeling, Phys. Rev. Lett. **82**, 2872 (1999).
14. I.M. Sokolov, R. Reigada, Phys. Rev. E **59**, 5412 (1999).
15. I.M. Sokolov, Phys. Rev. E **60**, 5528 (1999).
16. I.M. Sokolov, A. Blumen, J. Klafter, Europhys. Lett. **47**, 152 (1999).
17. R. Reigada, A.C. Martí, I.M. Sokolov, F. Sagués, J.M. Sancho, Phys. Rev. E **62**, 4997 (2000).
18. I.M. Sokolov, J. Klafter, A. Blumen, Phys. Rev. E, **61**, 2717 (2000).